# COMPARISON OF SELECTED PARAMETERS FOR EVALUATION OF RAIL SURFACE DAMAGE INTENSITY

JIŘÍ ŠLAPÁK*, TOMÁŠ MICHÁLEK

*University of Pardubice, Faculty of Transport Engineering, Department of Transport Means and Dignostics, Studentská 95, 532 10 Pardubice, Czech Republic*

* corresponding author: `jiri.slapak@upce.cz`

ABSTRACT. This paper deals with the issue of evaluation of a rail surface damage (*RSD*) intensity. Some ways of calculating parameters that represent the *RSD* are described. In this context, a multi-body model of a railway vehicle was created and several simulations of this model on a curved track were performed. Furthermore, these simulations were evaluated and the *RSD* parameters were compared.

KEYWORDS: Wheel/rail interaction, rail surface damage, wear number, multi-body simulation.

## 1. INTRODUCTION

In recent years, some railway infrastructure managers have started to use vehicle ratings based on damaging effects of vehicles on tracks. These damaging effects are directly related to maintenance requirements of tracks. One of the damaging effect is the rail surface damage (*RSD*), which occurs when wheels roll on rails. *RSD* primarily represents a wear of rails by abrasion and secondarily a relationship between the wear and a rolling contact fatigue (*RCF*). This method of evaluation may motivate vehicle operators to use and purchase track-friendly vehicles.

This paper is focused on several methods for evaluating *RSD* intensity and these methods are compared. These evaluation methods are described. The parameters that represent *RSD* intensity are compared depending on selected vehicle parameters. By means of multi-body simulations of vehicle running, a quantification of the parameters representing *RSD* intensity and damaging effects can be performed.

## 2. RAIL SURFACE DAMAGE

Rolling of wheels on rails is possible due to normal forces acting in wheel/rail contact areas and the existence of adhesion in these contact areas. In general, when wheels rolls on rails, creepages and tangential (creepage) forces occur in the wheel/rail contact areas. The creepages occur in the longitudinal and lateral directions and also as a spin (rotation around the vertical axis). The longitudinal creepage is primarily related to traction and braking forces and also to the conditions of the wheelset/track interaction (specifically on the delta-r function) in curves. The increase in the lateral creepage is caused by an increase in the angle of attack of the wheelset. The spin is related to the inclination of the wheel/rail contact area.

Creepages and spin result in tangential (creepage) forces and spin moment that cause loading of the rail surface. Due to this loading, the rail surfaces are damaged. In more detail, the issue of creepage forces is described in [1].

The first damaging effect is the wear of the rails and wheels by abrasion. The amount of wear depends on some design parameters of a vehicle, some wheel/rail contact conditions (coefficient of friction/adhesion, materials) and some track parameters.

The rolling contact fatigue (*RCF*) is another damaging effect caused by wheels rolling on rails. *RCF* causes cracks on the rail surface. Under certain conditions, crack initiations can be removed by wear on the rail surface. Thus, the wear can be beneficial in terms of the rolling contact fatigue.

### 2.1. WEAR NUMBER

The parameter called the wear number $T_\gamma$ [Nm/m] is the first option for evaluating and comparing the damaging effects of vehicles that result in *RSD*. This parameter is based on the physical assumption that the wear of the rails and wheels is caused by friction work performed in the wheel/rail contact. According this assumption, the wear number is defined as:

$$T_\gamma = |T_x \gamma_x| + |T_y \gamma_y|, \tag{1}$$

where $T$ [N] is the tangential (creepage) force and $\gamma$ [−] is the creepage in the wheel/rail contact. The letters $x$ and $y$ describe the longitudinal and lateral direction of these quantities. Equation 1 applies when spin and spin moment are neglected.

Since these quantities (specifically creepages and lateral creepage force) cannot be measured on a real vehicle, it is necessary to determine the value of the wear number using multi-body simulations of vehicle running.

The wear number presented in Equation 1 corresponds to the specific friction work performed in the wheel/rail contact. Furthermore, the wear number in this form is used in the methodologies of some railway infrastructure managers for setting track acess charges (e.g. methodology [2]).

**2.1.1.** RCF PREDICTION METHOD BASED ON $T_\gamma$

The wear number $T_\gamma$ is also used in the *RCF* prediction method. The non-linear dependence of the wear number and the so-called *RCF* damage index is shown in Figure 1 and described in [3]. This index indicates whether the rails are damaged due to wear, *RCF* or a combination of both, which is more common option. According to Figure 1:

- *RCF* damage index increases from 0 to $1 \cdot 10^{-5}$ as the wear number values incease from 15 N to 65 N. When the wear number value is 65 N, the probability of *RCF* crack initiation is greatest.

- Then the index value decreases to 0 as the wear number increases to 175 N. In this part, a wear begins to predominate over *RCF*.

- For the wear number values greater than 175 N, the *RCF* damage index has negative value. This mean that only wear damage occurs.
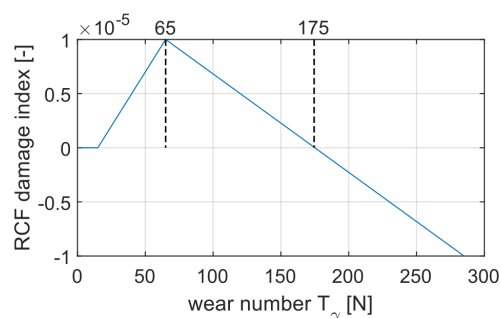


FIGURE 1. Dependence of the wear number $T_\gamma$ and *RCF* damage index. [3]

Figure 1 applies to R260 steel. For other steels, the position of the characteristic points differs.

**2.2.** RAIL SURFACE DAMAGE PARAMETER ACCORDING TO EN 14363

In the standard EN 14363 [4], the current evaluation of rail load in lateral direction is performed using the quatistatic lateral guiding force $Y_{a,qst}$. This force is also used as indirect evaluation parameter for the rail surface damage intensity especially the wear of rails, but sometimes it shows a very weak connection with *RSD*.

Another parameter for the evaluating of the rail surface damage intensity is presented in Annex K of standard EN 14363 [4]. The standard proposes the parameter $T_{qst}$ which is a combined quantity of lateral $Y_{qst}$, longitudinal $T_{x,qst}$ and vertical $Q_{qst}$ forces acting in the wheel/rail contact and represents the rail surface damage intensity. The parameter $T_{qst}$ is defined as:

$$T_{qst} = \frac{Q_{qst}}{10000} \cdot \left(330 \cdot f^2 - 62 \cdot f + 4\right), \qquad (2)$$

where

$$f = \frac{Y_{qst}}{Q_{qst}} + 0,62 \cdot \frac{|T_{x,qst}|}{Q_{qst}}. \qquad (3)$$

The constants in these equations are derived as regression parameters from the dependence of $T_{qst}$ and $T_\gamma$. The parameter $f$ (Equation 3) is dimensionless then the unit of the parameter $T_{qst}$ (Equation 2) is Newton [N]. This parameter has been defined in order to be able to measure the values of input parameters (forces) on a real vehicle without multi-body simulation.

Compared to the guiding force $Y_{a,qst}$, the parameter $T_{qst}$ better includes the influence of friction conditions in the wheel/rail contact area. The parameter $T_{qst}$ has only been defined for the guiding wheel of a vehicle.

**3.** MULTI-BODY SIMULATIONS

The values of previously defined quantities were obtained from multi-body simulations of running vehicle. The model and multi-body simulations of railway vehicle running were performed using SIMPACK simulation software.

**3.1.** MODEL OF RAILWAY VEHICLE

For the purposes of this study, the multi-body model of a conventional passenger car of an electric unit was used. The fundamental parameters of this model are listed in Table 1.

| Parameter | Value | Unit |
|---|---|---|
| Nominal mass of the carbody | 40000 | kg |
| Mass of the bogie frame | 5200 | kg |
| Mass of the wheelset | 2100 | kg |
| Bogie distance | 19 | m |
| Nominal bogie wheelbase | 2.4 | m |
| Vertical stiffness of the primary spring (per wheel) | 1.6 | kN/mm |
| Vertical stiffness of the secondary spring (per side of bogie) | 0.7 | kN/mm |

TABLE 1. Fundamental parameters of the multi-body model of the railway vehicle.

Setting the wheel/rail contact conditions is a very important part of the simulations. The wheel profile ORE S1002 and the rail profile 60E1 were used. The rail inclination of 1:40 was considered. The nominal friction coefficient value 0.4 was chosen. The FASTSIM algorithm was chosen to calculate the tangential (creepage) forces.
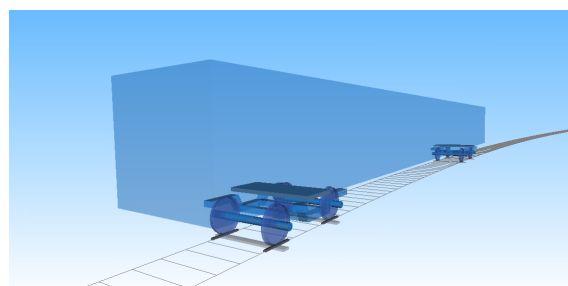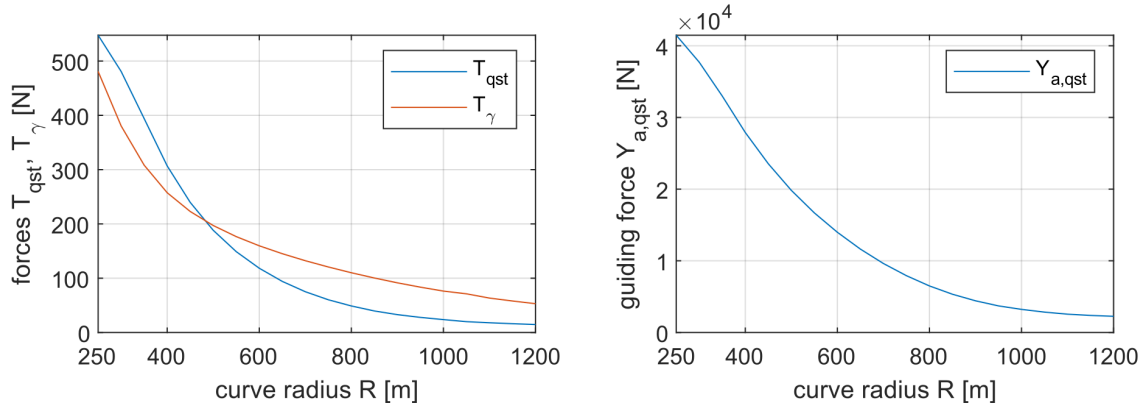


FIGURE 2. The vehicle model created in SIMPACK.

FIGURE 3. Basic comparison of the mentioned parameters used to evaluate *RSD* intensity depending on the curve radius *R*. Only for the guiding wheel on vehicle.

## 3.2. Track conditions

The simulations were performed on several curved tracks with a radius from 250 m to 1200 m. The length of the curve was set to 600 m. The cant $D$ and cant deficiency $I$ values are constant for all simulations.

- $D = 150$ mm
- $I = 130$ mm

According to these conditions, the vehicle speed was set in the range of values from 77 km/h to 169 km/h. In the order to consider a real model of the track, reference track irregularities were used and a model of elastic track foundation was created.

## 4. Simulation results

Time records of the quantities acting in the wheel/rail contact (lateral, longitudinal and vertical forces) and the parameter wear number $T_\gamma$ were monitored and exported from the multi-body simulations. From these records, the mean values of the quantities in the fully curved part of the tracks were calculated. The exported data from simulations were processed in MATLAB.

Because the parameters $T_{qst}$ and $Y_{a,qst}$ are defined for the guiding wheel of a vehicle, all comparisons and evaluations have been processed for the guiding wheel only.

## 4.1. Comparison of evaluation parameters

For the first look at the comparison of the mentioned RSD intensity parameters $(T_\gamma, T_{qst}, Y_{a,qst})$, the parameter values depending on the curve radius are plotted in Figure 3. This figure only shows the situation on the guiding wheel of vehicle for the nominal setting of the multi-body model and the simulation.

According to Figure 3, all *RSD* intensity parameters depending on the curve radius have the same trend and the shapes of the graph curves are similar. The values of the parameters progressively increase as the curve radius decreases. The figure further shows that the parameter $T_{qst}$ values are smaller than the

wear number $T_\gamma$ values in curve radii greater than 700 m. Then for smaller values of the curve radii, the parameter $T_{qst}$ values are greater then the values of the wear number $T_\gamma$. However, this only applies to the guiding wheel of the vehicle.

Figure 3 further shows that the curve of the wear number $T_\gamma$ has a convex character in the whole range of curve radii. This also applies to the parameter $T_{qst}$, except for the situation of the very small curve radius where the curve begins to be concave.

## 4.2. Influence of selected parameters

According to the standard EN 14363 [4], the formula for the parameter $T_{qst}$ (Equation 2) was defined for a wide range of selected operating conditons of a vehicle. Therefore, vehicle running simulations were performed with a focus on the influence of these parameters:

- friction coefficient in the wheel/rail contact $\mu$,
- weight of vehicle body $m$,
- bogie wheelbase $2a$,
- longitudinal stiffness of wheelset guiding $k_x$ per one wheel.

For all these parameters, the dependences of $T_{qst}$ and $T_\gamma$ on the curve radius $R$ are plotted in graphs. To compare of RSD intensity parameters, the difference between $T_{qst}$ and $T_\gamma$ is defined and calculated as:

$$T_\gamma - T_{qst} \quad [N]. \tag{4}$$

Furthermore, the relative difference is defined and calculated as:

$$(T_\gamma - T_{qst})/T_\gamma \cdot 100 \quad [\%]. \tag{5}$$

### 4.2.1. Influence of friction coefficient

In the first part, the influence of the friction coefficient values in the wheel/rail contact was investigated. Friction coefficient values of 0.2, 0.4 and 0.6 were selected.

Figure 4 shows comparison of the wear number $T_\gamma$ and the parameter $T_{qst}$ (calculated according to [4]) on the guiding wheel of the vehicle. For different

values of the friction coefficient $\mu$ in the wheel/rail contact area, the individual curves are plotted as a function of the curve radius $R$.

For all investigated values of the friction coefficient, this figure shows that the values of the parameter $T_{qst}$ are very close in the range of the curve radius from 700 m to 1200 m. This behavior of the parametr $T_{qst}$ is different from the wear number $T_\gamma$. Further, as the curve radius value decreases, the values of the parameter $T_{qst}$ as well as the parameter $T_\gamma$ values increase.
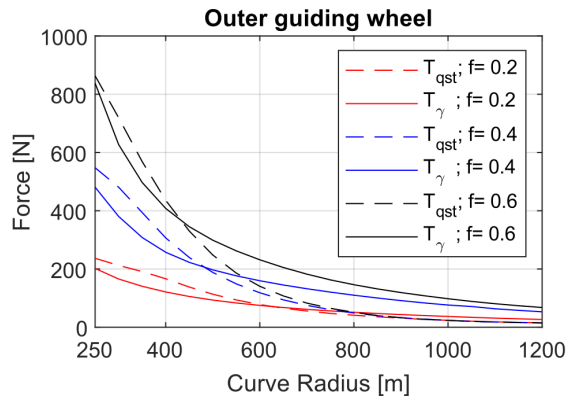


FIGURE 4. Dependence of the $T_{qst}$ and $T_\gamma$ on the curve radius $R$ in defined range of the friction coefficient values $\mu$.

Figure 4 shows that the friction coefficient value in the wheel/rail contact area has a great influence on the values of wear number $T_\gamma$ and also shows that the parameter $T_{qst}$ follows this trend.
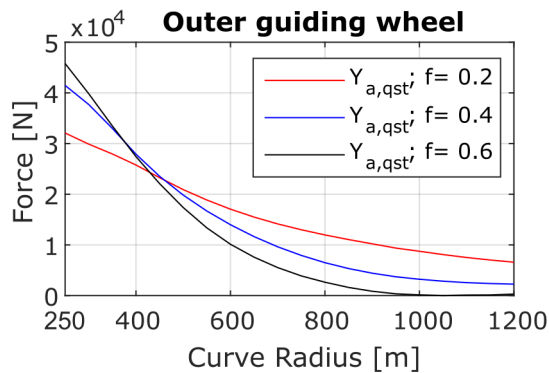


FIGURE 5. Dependence of the $Y_{a,qst}$ on the curve radius $R$ in defined range of the friction coefficient values $\mu$.

In Figure 5, the influence of the friction coefficient $\mu$ on lateral guiding force $Y_{a,qst}$ is shown. As the friction coefficient values increase, the slope of the plotted curves increases. This behavior is the same as for the parameters in Figure 4. But the curves are shifted, which causes a large mismatch between the force $Y_{a,qst}$ and the parameters $T_{qst}$ and $T_\gamma$.

The next Figure 6 shows the difference and the relative difference between the values of the wear

number $T_\gamma$ and the parameter $T_{qst}$ in defined range of friction coefficient values. In general, the best match of these parameters occurs for the smallest value of the friction coefficient. But for very small curve radii, the value of the relative difference for the friction coefficient of 0.6 is the smallest. This mean that in very small curve radii, $T_{qst}$ corresponds better to the wear number $T_\gamma$ with increasing value of the friction coefficient. On the other hand, for large curve radii, the parameter $T_{qst}$ best corresponds to the wear number $T_\gamma$ under the conditions of the smallest value of the friction coefficient.

For a radius curve of 1200 m and a friction coefficient of 0.6, the value of the relative difference is 78%.
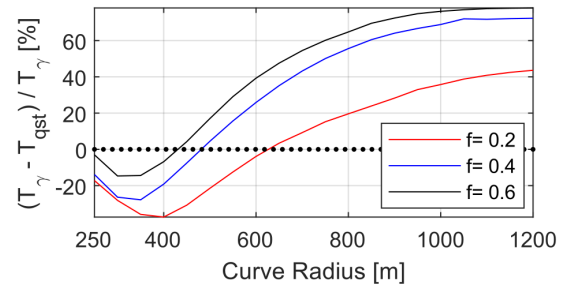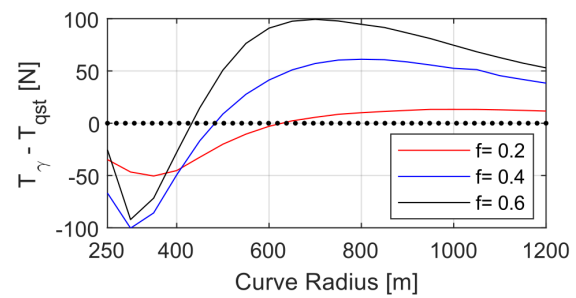


FIGURE 6. The difference $T_\gamma - T_{qst}$ depending on the curve radius $R$ (above) and the relative difference $(T_\gamma - T_{qst})/T_\gamma$ depending on the curve radius $R$ (below) in the defined range of friction coefficient $\mu$ values.

### 4.2.2. INFLUENCE OF VEHICLE WEIGHT

In the next part, the influence of the vehicle weight was investigated. For this evaluation, the vehicle body mass $m$ was set to 35, 40 and 45 tons.

Figure 7 shows the values of the parameter $T_{qst}$ and the wear number $T_\gamma$ as a function of the curve radius $R$ for the defined values of the vehicle body weight. According to this figure, the weight of vehicle has an effect on the wear number $T_\gamma$ values. This effect is most evident for the small curve radii. On the other hand, the values of the parameter $T_{qst}$ do not change when the vehicle weight changes. This applies in whole range of the curve radii expect the very small curve radii.
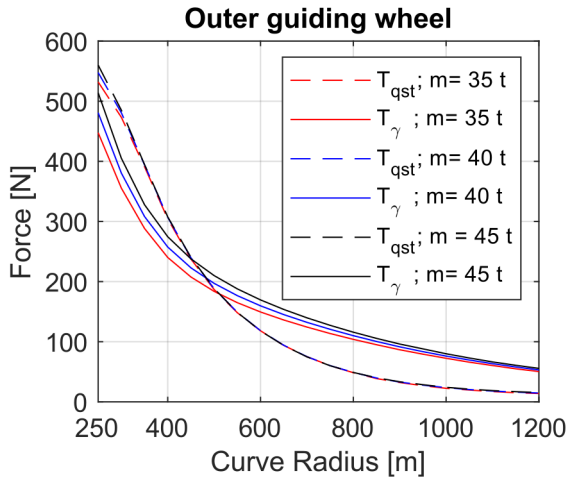
FIGURE 7. Dependence of the $T_{qst}$ and $T_\gamma$ on the curve radius $R$ for defined values of the vehicle body mass $m$.
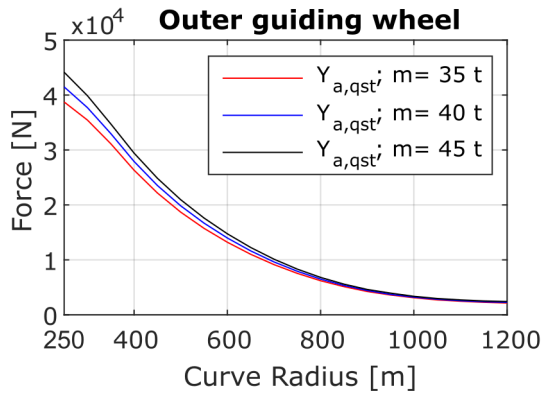


FIGURE 8. Dependence of the $Y_{a,qst}$ on the curve radius $R$ for defined values of the vehicle body mass $m$.

Figure 8 shows that the weight of the vehicle body has an effect on the guiding force $Y_{a,qst}$. The wear number $T_\gamma$ (in Figure 7) has a similar effect. Furthermore, the dependence of the force $Y_{a,qst}$ on the curve radius is concave in very small curve radii, as well as the dependence of the parameter $T_{qst}$ on the curve radius.

In Figure 9, the difference and the relative difference of the parameters $T_{qst}$ and $T_\gamma$ are shown in relation to Figure 7. In very small curve radii, the best match of the investigated parameters occurs at higher values of the vehicle weight. Then in the large curve radii, the best match of the parameters occurs for the lightest vehicle but the differences disappear in very large curve radii.

In the value of the curve radius of 1200 m, the relative difference value is 72% and this value does not depend on the vehicle weight.
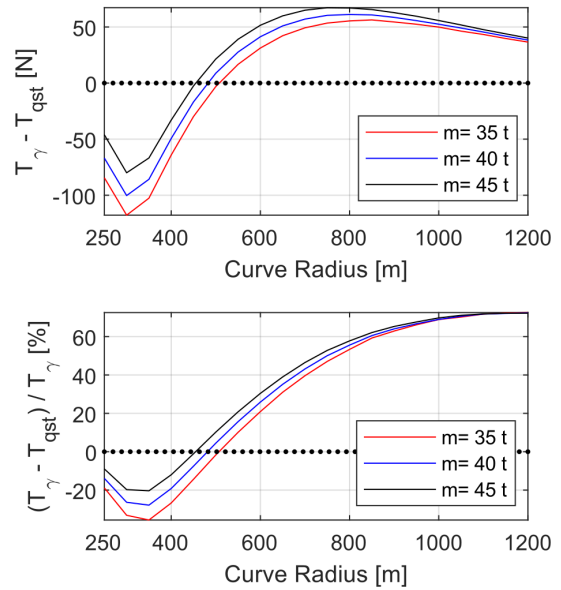


FIGURE 9. The difference $T_\gamma - T_{qst}$ depending on the curve radius $R$ (above) and the relative difference $(T_\gamma - T_{qst})/T_\gamma$ depending on the curve radius $R$ (below) for defined values of the vehicle body mass $m$.

**4.2.3.** INFLUENCE OF BOGIE WHEELBASE

In this part the influence of the bogie wheelbase $2a$ on the parameters $T_{qst}$ and $T_\gamma$ is analyzed. The value of the bogie wheelbase was set to 2.0, 2.4 and 2.8 meters.
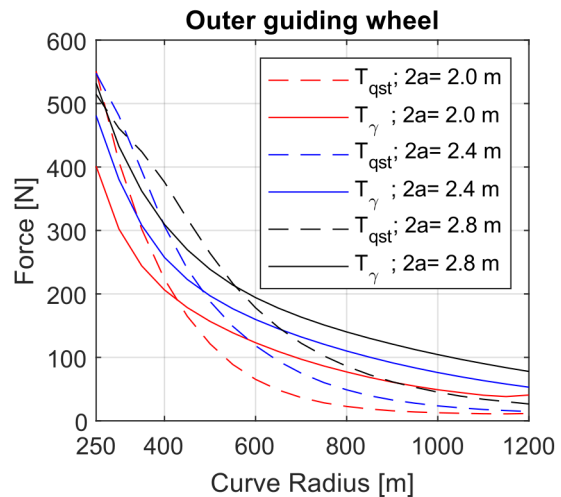


FIGURE 10. Dependence of the $T_{qst}$ and $T_\gamma$ on the curve radius $R$ for defined values of the bogie wheelbase $2a$.

In Figure 10, the influence of the bogie wheelbase values is evident for both parameters of RSD intensity over the whole range of the curve radii. Again, the values of $T_{qst}$ are smaller than the values of $T_\gamma$ for large curve radii. Then, for small curve radii, the values of $T_{qst}$ increase over the values of $T_\gamma$.
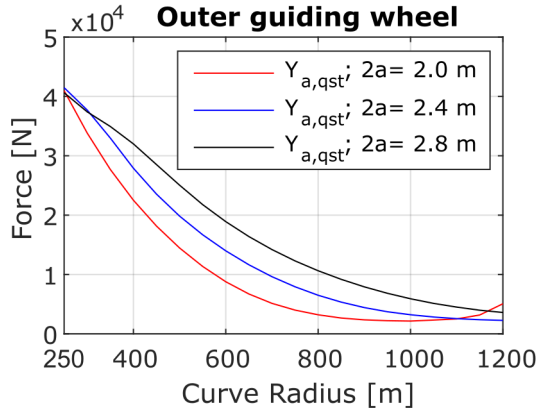
FIGURE 11. Dependence of the $Y_{a,qst}$ on the curve radius $R$ for defined values of the bogie wheelbase $2a$.

According to Figure 11, the influence of the bogie wheelbase $2a$ on the guiding force $Y_{a,qst}$ values and on the parameter $T_{qst}$ is similar. For large and very small curve radii, it is difficult to predict and describe the values of the force $Y_{a,qst}$ .

The dependence of the $T_\gamma$ values on the curve radius has the same trend for different values of bogie wheelbase. This does not apply to the parameter $T_{qst}$ whose trends are changing in the very small curve radii. This is also shown in Figure 12 where the both differences increase (in terms of absolute values) in the very small curve radii under the condition of the bogie wheelbase of 2.0 m. But for the other values of the bogie wheelbase in the very small curve radii, the differences decrease with decreasing the curve radius.
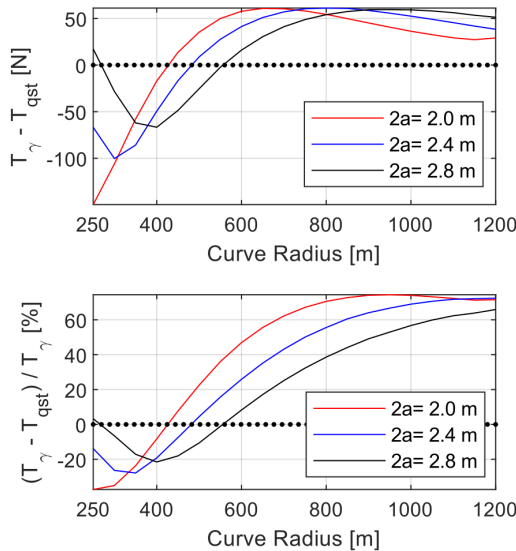


FIGURE 12. The difference $T_\gamma - T_{qst}$ depending on the curve radius $R$ (above) and the relative difference $(T_\gamma - T_{qst})/T_\gamma$ depending on the curve radius $R$ (below) for defined values of the bogie wheelbase $2a$.

In general, Figure 12 shows that the best match

between the $T_{qst}$ and $T_\gamma$ parameters occurs for the vehicle with the longest bogie wheelbase.

According to the first graph in Figure 12 and for the curve radius of 250 m, the value of the difference is 150 N for the vehicle with bogie wheelbase of 2.0 m. It is the highest value of the absolute diference of the RSD intensity parameters. But from the point of view of the relative difference of these parameters, the value corresponds to the relative difference of 37%. A much larger relative difference occurs in curve radius of 950 m where the value is about 74% and it is the highest value of the relative difference of the parameters for this analysis.

**4.2.4.** INFLUENCE OF LONGITUDINAL STIFFNESS OF WHEELSET GUIDING

The influence of the longitudinal stiffness of the wheelset guiding $k_x$ per one wheel on the parameter $T_{qst}$ and the wear number $T_\gamma$ is the last analyzed part. The values of the longitudinal stiffness of the wheelset guiding per one wheel were set to $2.0 \cdot 10^7$, $3.5 \cdot 10^7$ and $5.0 \cdot 10^7$ N/m.
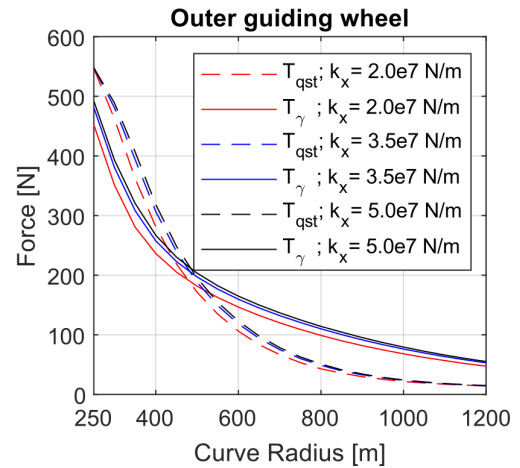


FIGURE 13. Depenence of the $T_{qst}$ and $T_\gamma$ on the curve radius $R$ in defined range of the longitudinal stiffness of wheelset guiding $k_x$ per one wheel.
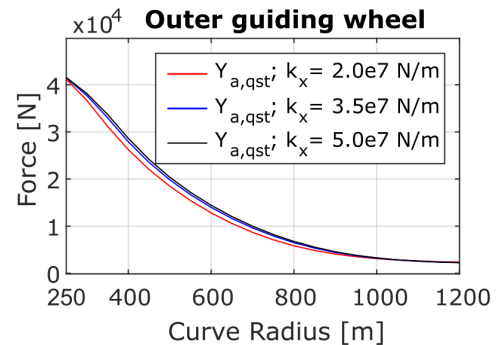


FIGURE 14. Depenence of the $Y_{a,qst}$ on the curve radius $R$ in defined range of the longitudinal stiffness of wheelset guiding $k_x$ per one wheel.

Figure 13 shows that the longitudinal stiffness of the wheelset guiding in defined range of values has

a small effect (in comparison with other investigated parameters) on the values of the parameter $T_{qst}$ and the wear number $T_\gamma$. From this point of view, the behavior of these parameters is the same. Thus, in general, changing the stiffness value causes the same reaction in the parameter $T_{qst}$ as in the wear number $T_\gamma$.

According to Figure 14, the behavior of the dependence of the guiding force $Y_{a,qst}$ on the curve radius is the same as the dependences on Figure 13. This means that the effect of the longitudinal stiffness of wheelset guiding $k_x$ in a defined range of values on the guiding force $Y_{a,qst}$ values is small.
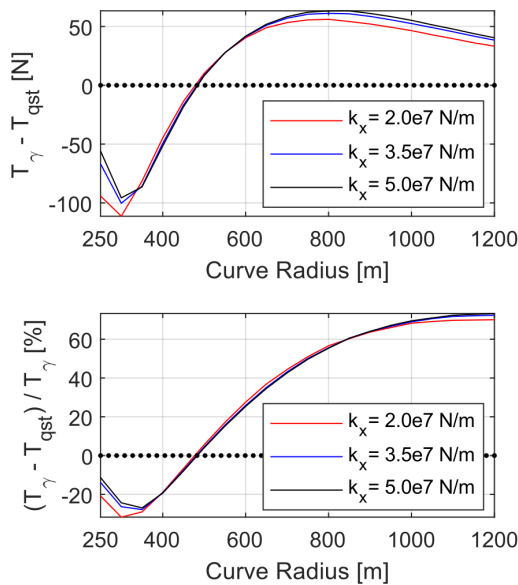


FIGURE 15. The difference $T_\gamma - T_{qst}$ depending on the curve radius $R$ (above) and the relative difference $(T_\gamma - T_{qst})/T_\gamma$ depending on the curve radius $R$ (below) in the defined range of the longitudinal stiffness of wheelset guiding $k_x$ per one wheel.

This fact is confirmed in Figure 15. This figure shows that the difference and the relative difference values are almost identical for the defined range of the longitudinal stiffness values. Some effect of the longitudinal stiffness to the difference and the relative difference of RSD intensity parameters occurs in very small curve radii.

## 5. Conclusions

It can be assumed that the wear number $T_\gamma$ represents the wheel and rail abrasion wear and indirectly also represents the rolling contact fatigue effects. It is used by railway infrastructure managers as an indicator of damage and maintenance requirements of a curved track. Unfortunately, the wear number must be obtained from multi-body simulations and cannot be measured on a real vehicle. This fact means a risk that the results of the multi-body simulations can be affected by the model settings. The correctness of this settings cannot be experimentally verified.

The lateral guiding force $Y_{a,qst}$ is a parameter that is used to evaluate the lateral load of the rails. This force exhibits similar behavior and trends as the wear number $T_\gamma$ depending on the curve radius, but its values are different. For the reason, an alternative quantity, the parameter $T_{qst}$ is defined in the standard EN 14363.

Based on multi-body simulations of running a conventional passenger four-axle railway vehicle, it was found that the parameter $T_{qst}$ shows the same trends as the wear number $T_\gamma$ on the outer guiding wheel of a vehicle. However, there are differences between the values of these parameters, which vary depending on the curve radius. The parameter $T_{qst}$ values are smaller than the wear number values in the large curve radii. Conversely, the parameter $T_{qst}$ values are higher than the wear number in the very small curve radii. The best match of these parameters occurs in curve radii from 400 to 600 meters. The worst match occurs in the very large curve radii where the relative difference between the parameter $T_{qst}$ and the wear number $T_\gamma$ has a value higher than 70 percent. This mean that this approximation of the parameter $T_{qst}$ is bad for very large curve radii.

The friction coefficient value in the wheel/rail contact area has the greates influence on the RSD intensity parameters. Further, the vehicle body weight affects the wear number values, but has almost no effect on the parameter $T_{qst}$ value. The values of the longitudinal stiffness of wheelset guiding have the same effect on both RSD intensity parameter.

The defined parameter $T_{qst}$ for evaluation of RSD intensity follows the trend of the wear number. But between these parameters, there is bad match in the large curve radii and the parametr $T_{qst}$ does not respond to the vehicle weight change. The parameter $T_{qst}$ can represent the wear number, but the accuracy of this parameter could be improved.

## References

[1] Voltr, P.: Calculation of locomotive traction force in transient rolling contact. In: Applied and Computational Mechanics, 11, 69-80, 2017.

[2] Feredal Office of Transport. Base Price Wear in the train-path pricing system 2017 – Instruction for determining vehicle prices. Bern, 2017.

[3] Iwnicki, D. S.: The Effect of Profiles on Wheel and Rail Damage. In: International Journal of Vehicle Structures & Systems,1(4), 99-104, 2009.

[4] EN 14363:2016+A1:2018. Railway applications – Testing and Simulation for the acceptance of running characteristics of railway vehicles – Running behaviour and stationary tests. Brusel: European Committee for Standardization, 2018.